Available online at www.CivileJournal.org

Civil Engineering Journal

(E-ISSN: 2476-3055; ISSN: 2676-6957)

Vol. 8, No. 01, January, 2022

Out-of-Plane Strengthening of Unreinforced Masonry Walls by Glass Fiber-Reinforced Polyurea

Hye-Sook Jang [1], Jae-Hyoung An [1], Jun-Hyeok Song [1], Seung-Hwan Son [1], Yu-Sik Hong [1], Hee-Chang Eun [1*]

[1] *Department of Architectural Engineering, Kangwon National University, Chuncheon, 24341 Korea.*

Received 28 August 2021; Revised 08 November 2021; Accepted 29 November 2021; Published 01 January 2022

Abstract

Fiber-reinforced polymer reinforcement or polyurea reinforcement techniques are applied to strengthen unreinforced masonry walls (UMWs). The purpose of this experimental study is to verify the out-of-plane reinforcing effect of sprayed glass fiber-reinforced polyurea (GFRPU), which is a composite elastomer made of polyurea and milled glass fibers on UMW. The out-of-plane strengths and ductile behaviors based on various coating shapes are compared in this study. An empirical formula to describe the degree of reinforcement on the out-of-plane strength of the UMW is derived based on the experimental results. It is observed that the peak load-carrying capacity, ductility, and energy absorption capacity gradually improve with an increase in the strengthening degree or area. Compared with the existing masonry wall reinforcement method, the GFRPU technique is a construction method that can help improve the safety performance along with ease of construction and economic efficiency.

Keywords: Glass Fiber-Reinforced Poloyurea; Out-of-Plane Reinforcement; Strengthening; Ductility; Energy Absorption Capacity; Unreinforced Masonry Wall.

1. Introduction

In terms of the durability of existing buildings, several attempts have been made to improve their lifespan by performing repair and reinforcement. As nonstructural elements, unreinforced masonry walls (UMWs) have low bending resistance and brittle fracture patterns. Considering the effects of lateral forces such as earthquakes and wind loads, UMWs should be designed to resist in-plane lateral loads as well as out-of-plane loads. Darbhanzi et al. [1] reported the reinforcement effect of vertical steel ties to enhance the strength and ductility of UMWs. Recently, fiber-reinforced polymer (FRP) reinforcement or polyurea reinforcement have been proposed in place of steel plates to resist lateral forces. Research related to the improvement of out-of-plane strength is based on explosion-proof reinforcement design. FRP and polyurea reinforcement methods are the two main reinforcement methods used for out-of-plane reinforcement, and other techniques include reinforcement using polyurethane, steel plate, and aluminum foam [2].

The FRP technique is more durable than reinforcement using reinforcing bars, and has the advantage of light weight and capability of being processed into various geometric shapes. FRP reinforcement significantly improves the strain and ductility. Myers and Tanizawa [3] reported that the improvement was significant, up to three times. Hrynyk and Myers [4] reported that polyurea coating can improve the energy absorption capacity of masonry filling walls and reduce wall

* Corresponding author: heechang@kangwon.ac.kr

http://dx.doi.org/10.28991/CEJ-2022-08-01-011

delamination. It was found that reinforcement using the FRP lattice and polyurea composite elastomer was destroyed prematurely owing to insufficient bonds between the wall and the surrounding structure. The authors developed an analysis model simplified by arch behavior to estimate the degree of reinforcement of the out-of-plane strength with FRP. Galati et al. [5] presented design guidelines for the strength of polyurea reinforced with glass grids, FRP laminates, and masonry structures reinforced with FRP bars. Salem et al. [6] evaluated the out-of-plane behavior of reinforced masonry shear walls with different parameters. Turkmen et al. [7] studied out-of-plane retrofitting technique for clay brick masonry buildings by carbon fiber reinforced polymer (CFRP) strips. Meriggi et al. [8] proposed the out-of-plane strengthening method of masonry walls by fabric reinforced cementitious matrix. Corradi et al. [9] investigated the out-of-plane reinforcement by high-strength steel cables fully embedded in the mortar bed joints. Guerreiro et al. [10] developed a strengthening technique by CFRP layer to masonry walls.

Polyurea, an elastomer, has excellent deformability and energy absorption capacity [11]; therefore, it is an explosion-proof material that can improve the structural performance of non-structural elements. Unlike the existing manual lamination method, a polyurea reinforcement method was introduced to save time and labor. The UMW has a low out-of-plane resistance owing to its low bending resistance and mechanical properties owing to which it can be fractured by brittleness. Broekaert [12] demonstrated that polyurea is a material with high hardness, flexibility, fracture and tensile strength, and chemical and water resistance. It has been reported that polyurea can be further reinforced by adding nanoparticles with different properties. Hrynyk and Myers [13] confirmed that reinforcement through a lattice-type polymer attached to polyurea can improve the out-of-plane loading capacity and ductility and reduce exfoliation. Using FRP and polyurea, elongated fibers were added to improve the tensile strength of polyurea and shear resistance to the masonry filling wall under the impact of an in-plane load. Researchers at Missouri University of Science and Technology led to the proposal of a reinforcing method through the application of discrete fiber-reinforced polyurea (DFRP). The effectiveness of DFRP under seismic conditions and its ductility was verified through DFRP-reinforced concrete cylinder experiments [14-17].

Polyurea reinforced with glass fiber-reinforced polymer (GFRP) was experimentally verified as an effective technique for reinforcing the walls of UMWs [18]. Myer and Tanizawa [3] conducted a study to verify the reinforcing effect of coating UMW with a composite elastomer made of polyurea and chopped E-type glass fibers as an external reinforcing material. Greene and Myers [17] investigated the effect of DFRP coating on the reinforcement capacity and ductility of concrete beams in bending and shear. In addition, an analytical model describing the bending behavior of polyurea was presented. Wu et al. [19] investigated the reinforcing effect based on the coating thickness and compared the reinforcement effect for nonreinforced and polyurea-reinforced clay brick walls against blast loads. The reinforcement effect on concrete beams and columns reinforced by glass fiber-reinforced polyurea (GFRPU) mixed with milled glass fiber to improve the tensile strength of polyurea [20-23] was investigated. The authors reported that GFRPU was effective in enhancing the strength and ductility of structural members. The in-plane reinforcement effect of GFRPU on masonry-filled walls [24] was investigated.

GFRPU, a new reinforcement construction method, is intended to be applied to the reinforcement of UMWs in the out-of-plane direction. Failure in the out-of-plane direction causes secondary damage, so this work investigates the utility of GFRPU to prevent it. In this study, the out-of-plane reinforcing effect of GFRPU on UMW is verified through experiments. The out-of-plane strength, ductility, and energy absorption capacities based on the various coating shapes are compared. The empirical formula used to describe the degree of out-of-plane reinforcement is derived from the experimental results. It was noticed that the peak load-carrying capacity, ductility, and energy absorption capacity gradually improve with an increase in the degree of strengthening. Compared with the existing masonry wall reinforcement method, reinforcement using GFRPU is a construction method that can be applied to the field to improve the safety performance accompanied with ease of construction and economic efficiency. A flowchart of this study is shown in Figure 1.

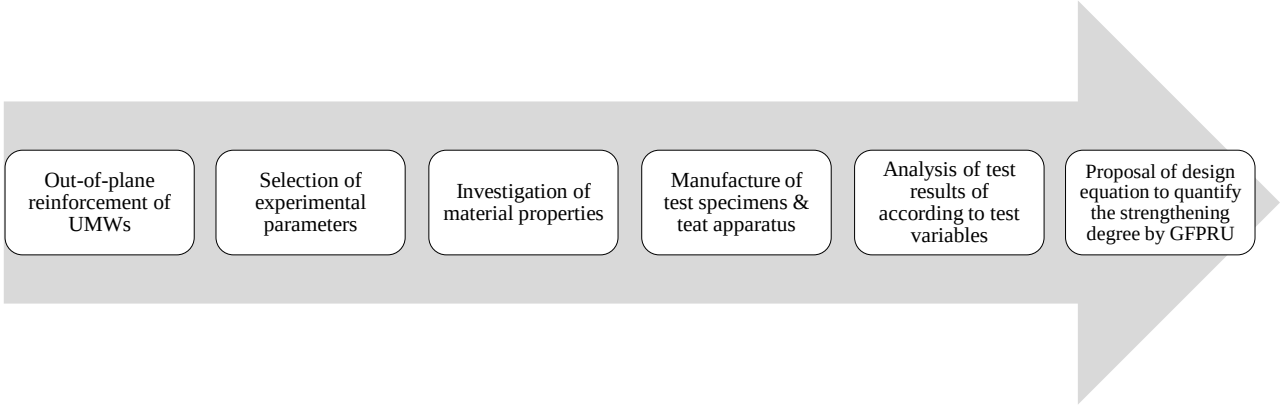

Figure 1. Flowchart of this study

2. Experiment

2.1. Material Properties

A mortar test specimen was prepared to measure its compressive strength. The specimen for the compressive strength test was produced simultaneously as the test specimens were constructed and cured for 28 day after production. The compressive strength test was carried out in accordance with the KS L 5105 standard for the compressive strength test method of hydraulic cement mortar, and the average compressive strength of the three specimens was measured to be 10.4 MPa.

Red clay bricks were used in this experiment for the exterior finishing of buildings. There are two methods for measuring the compressive strength of a unit brick and a masonry prism. The unit strength measurement method refers to the compressive strengths of the individual materials. The compressive strength of the clay bricks was tested based on the criterion for the test of the compressive strength of bricks in KS F 4004 and was measured to be 53.9 MPa. The physical properties of GFRPU were also investigated through experiments. Because it is not certain whether the added glass fiber is uniformly dispersed in the polyurea, 20 specimens were prepared to reduce the deviation of the experimental values, and the tensile strength was measured. It was reported in a previous study [24] that the optimum weight ratio of the milled glass fiber to polyurea for obtaining the peak tensile strength was approximately 5%, and this ratio was used for producing the GFRPU in this study.

A composite masonry prism was manufactured to determine the compressive strength of the design. The specimens were fabricated in a laboratory based on ASTM C1314 (a standard test method for the compressive strength of masonry prisms). After 28 day, an experiment was conducted to measure the strength of the masonry bricks (Figure 2). The measured compressive strength was corrected with respect to the aspect ratio. That is, the measured compressive strength was multiplied by the correction factor listed in Table 1 to determine the compressive strength. Four prism specimens were prepared, and the average compressive strength was measured to be 18.77 MPa.

Figure 2. Prism test of masonry bricks

Table 1. Correction factor according to shape ratio

Shape ratio	1.3	1.5	2.0	2.5	3.0	4.0	5.0
Correction factor	0.75	0.86	1.0	1.04	1.07	1.15	1.22

The tensile strength of GFRPU was measured in accordance with KS F 4922 “Polyurea resin waterproofing membrane coating.” The tensile strength was increased by approximately 36% from 22.73 to 30.96 MPa through the addition of glass fiber of weight ratio 5%, and the elastic modulus was also increased by approximately 44% from 99.89 to 143.9 MPa. The addition of glass fiber is a significant factor that increases the tensile strength and modulus of GFRPU. In contrast, because the added glass fiber replaced the corresponding volume of polyurea in GFRPU, it was noticed that the elongation rate decreased slightly from 418% to 362%. This leads to a slight decrease in tensile strain until fracture beyond the peak tensile strength. Despite a slight decrease in the elongation rate, the elongation rate was sufficient to delay the fracture or drop-off of the reinforced bricks.

2.2. Specimens

The test specimen reinforced by GFRPU was assumed to be a masonry wall of red clay bricks constructed on the exterior wall of the building. GFRPU was sprayed on the wall face 24 h after the wall surface was treated, and a primer was applied to improve the adhesion performance. The mixed GFRPU was sprayed on the surface of the specimen using a mechanical device meant for mixing polyurea and milled glass fibers.

A static test was conducted to evaluate the out-of-plane strength reinforced by the GFRPU coating. It was examined whether stability against static load was sustained instead of the destruction caused by earthquakes or dynamic loads. After laying the specimen horizontally, a uniform load was applied in the direction of gravity. The out-of-plane load was assumed to be a uniform load of the same magnitude rather than a concentrated load. The specimen was constructed using a wall with a length of 1300 mm, height of 1300 mm, and thickness of 190 mm with 1B stacking inside the steel frame, as depicted in Figure 3. The four edges of the specimen were supported by steel supports outside the 1100 mm×1100 mm net loading region.

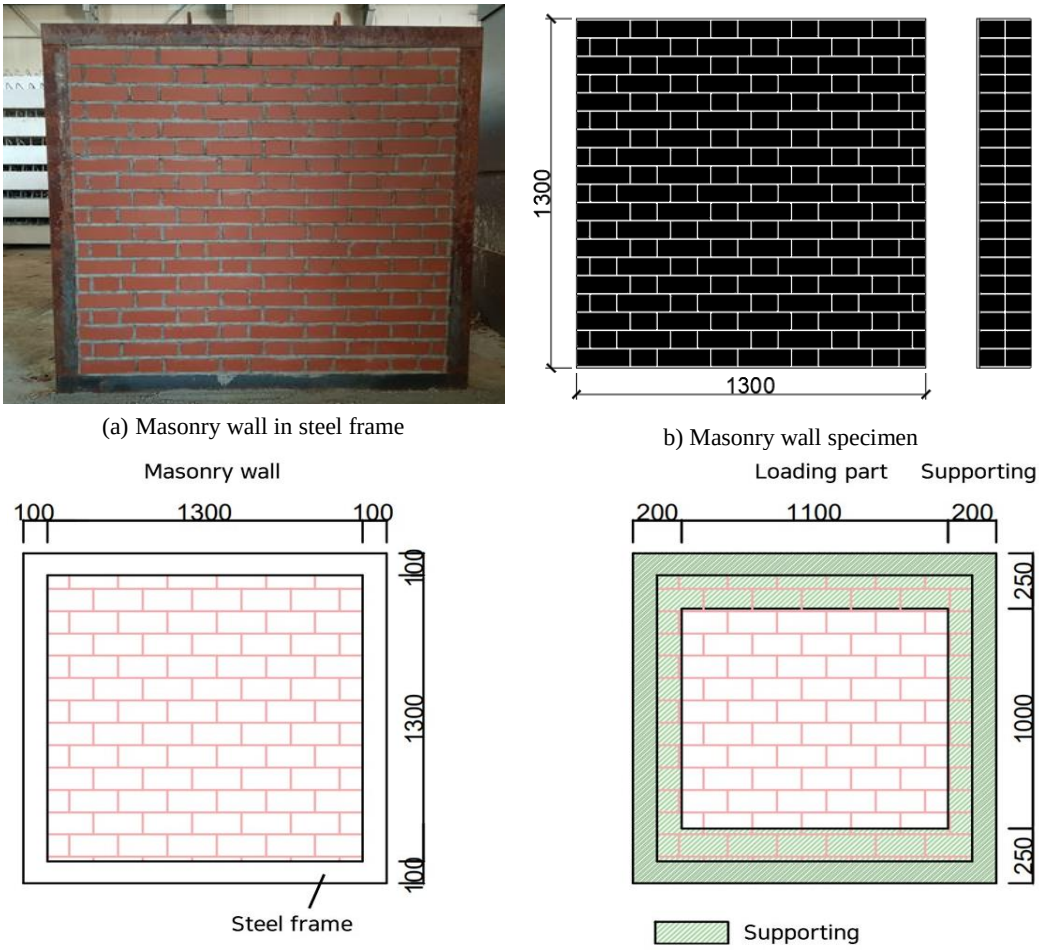

(a) Masonry wall in steel frame

b) Masonry wall specimen

c) Loading and supporting parts

Figure 3. Specimen and reinforcement by steel frame (unit: mm)

The reinforcement effect was investigated according to the reinforcement types, such as "X," "+," and "E," on one face of the wall (Figure 4). Here, "X" and "+" indicate X- and +-shaped coating, and "E" indicates the entire coating. The glass fiber contained in the GFRPU was 5% by weight ratio, and the spraying thickness of all the specimens was 5 mm, which was uniformly applied to one tensile surface.

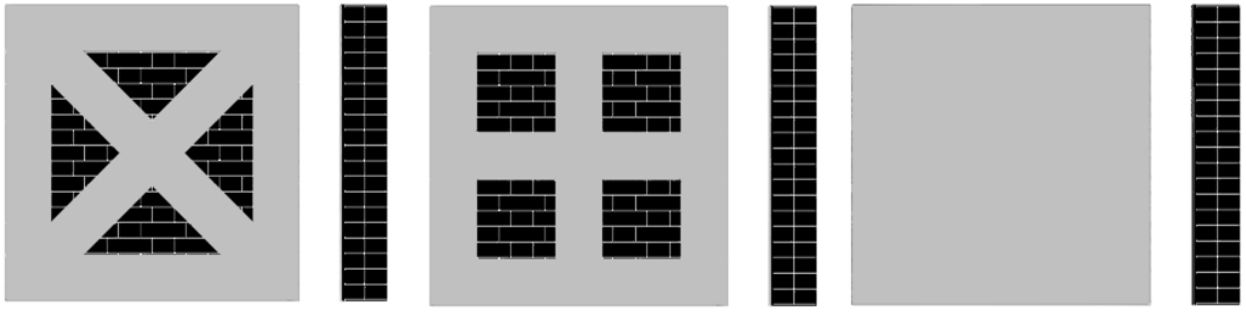

(a) X-type specimen b) +-type specimen c) Entire reinforcement specimen

Figure 4. Strengthening types of specimen

The loading was performed using a displacement control method (Figure 5) with a loading speed of 0.20 mm/min. The specimen was laid horizontally, and a steel plate was installed on top so that the load acting on the top of the specimen was uniformly applied to the masonry wall. The top refers to the compressed surface on which the GFRPU is not applied. It was difficult to determine the deformation shape of the masonry wall, such as cracks and deflections, at every incremental step of displacement. Because of the sprayed GFRPU, the appearance of cracks could not be seen with the naked eye, and there was no space or method to measure the deflection. However, the load–displacement relationship could be obtained by the force device through displacement control.

a) Photo of loading layout b) Loading on specimen

Figure 5. Specimen and loading test apparatus

The load was increased based on the increment in displacement, and the loading was stopped when the expected failure was reached. Although it was not possible to identify the damage or crack pattern of the specimen during loading, the mechanical behavior was evident from the load–displacement curves.

2.3. Failure Mode

Figure 6 depicts the failure modes of each specimen after the completion of the experiment. All the specimens were fractured after cracks occurred along the edges in contact with the support plate. It is predicted that the UMW should be rapidly destroyed along with cracks along the outer edge of the loading steel plate. Because of this risk of brittle fracture caused by rapid fracture, the UMW specimen was excluded from this experiment. The design formula of Equation 1 was used to calculate the out-of-plane strength specified in the Korean Code [25] instead of the experiment. The cracks or fractures on the GFRPU reinforcement specimens were rarely seen on the reinforced face. Deep cracks were seen with GFRPU peeling at the end edges of the loading plate at failure. The reinforced masonry wall surface could be maintained during loading, and the drop-off could be delayed owing to the excellent elongation of the GFRPU. The GFRPU confines the tensile surface of the masonry wall without cracking or delamination before fracture. The crack pattern on the reinforcement surface could hardly be seen because of the opaque GFRPU. Experiments have verified that the load-carrying capacity can be increased through additional reinforcement or fixation along the load-bearing surface, and the damage caused by the sudden drop-off can be prevented when applied to the exterior wall. The GFRPU reinforcement prevents a sudden collapse of the masonry wall in the event of an earthquake.

a) X-type specimen

b) +-type specimen

c) E-type reinforcement specimen

Figure 1. Failure modes

2.4. Load-Displacement Curves

Table 2 presents the peak load P_{peak} and the corresponding displacement of the specimen. The peak load was utilized as an index to evaluate the reinforcement effect of the GFRPU. It was seen that the +-type specimen retained the lowest peak load and strengthening effect of all specimens. However, the X-type specimen exhibited a higher peak load than the E-type specimen, despite the smaller sprayed area. The difference was caused by the inaccurate sprayed area and non-uniform thickness when the sprayed GFRPU was dispersed on the specimen. In the table, $P_{un,peak}$ represents the peak load of the unreinforced specimen calculated using Equation 1. The out-of-plane load-resisting capacity evaluated in this experiment was affected by the support conditions. The interface end edges up to 100 mm width of the specimen depicted in Figure 3-c were supported by the steel frame, unlike the actual masonry wall without an interface. Thus, the peak load measured in this experiment was corrected by multiplying it by 0.8, considering the end conditions. The corrected peak load is expressed by $P_{m,peak}$. The data presented in the table indicates that the peak out-of-plane strength increases by 16 to 50% owing to GFRPU reinforcement.

Table 1. List of loads and displacements at main steps

Specimens	Peak load (kN)	$P_{m,peak}$ (kN)	$P_{peak}/P_{un,peak}$	$P_{m,peak}/P_{un,peak}$	Displacement at peak load (mm)
X-type	643.7	515.0	1.87	1.5	3.30
+-type	500.2	400.2	1.45	1.16	7.56
E-type	627.3	501.8	1.82	1.46	6.48

* The peak load of unreinforced specimen calculated by Equation 1 is 344.4 kN.

The displacement at the peak load in Table 2 seems to have little effect on the degree of strengthening. This is explained by the load–displacement curves. Figure 7 depicts the relationship between the out-of-plane load and the corresponding displacement. After the initial loading, the initial stiffness of the X-type specimen was unexpectedly the largest, and it can be seen that the initial stiffness decreased in the order of E-type and +-type reinforcement specimens. In the case of the E-type and +-type reinforcement specimens, it is estimated that the stiffness decreased because the displacement increased unexpectedly because the displacement-measurement point slides during loading.

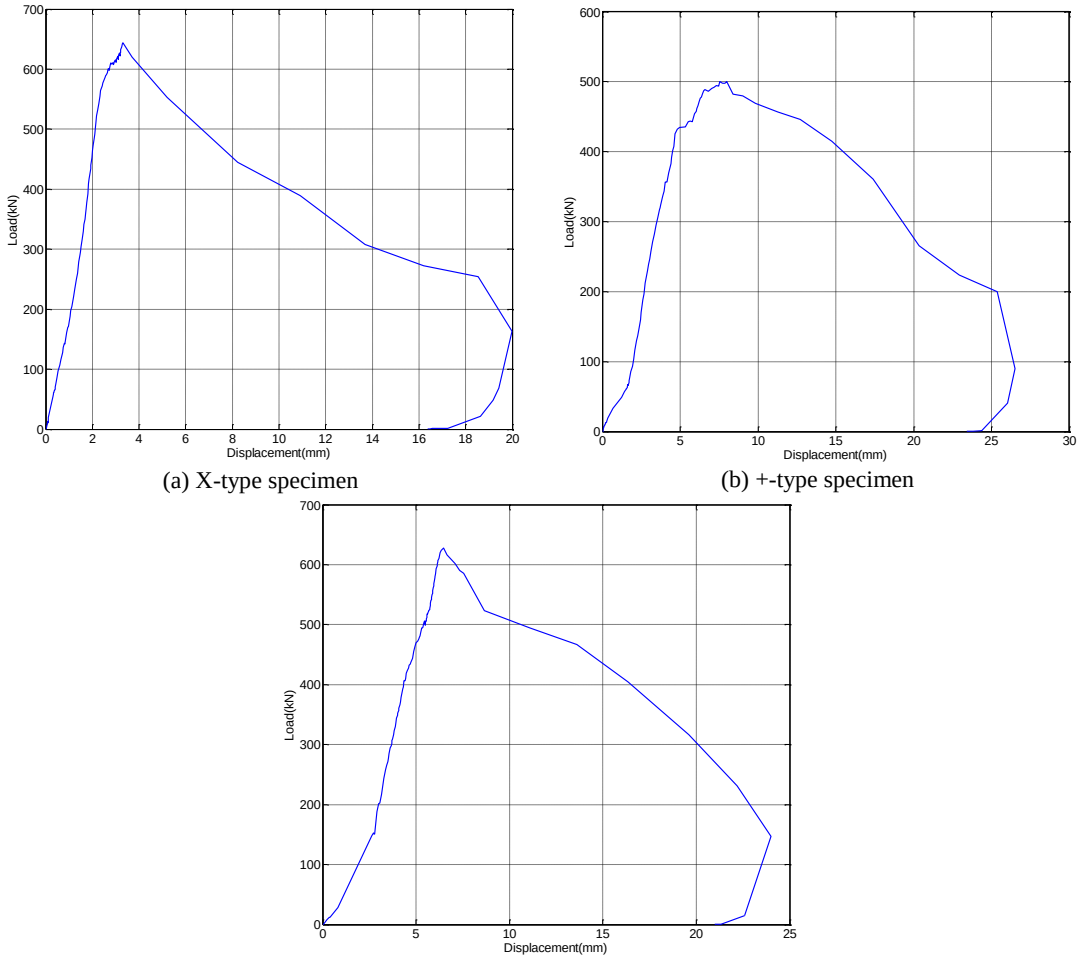

(a) X-type specimen

(b) +-type specimen

c) entire reinforcement specimen

Figure 2. Load-displacement curves

The specimens indicated ductile behavior owing to the elongation property of polyurea beyond the peak load. In the plots, it can be seen that the +-type specimen exhibits ductile behavior despite the lowest peak load. The X-type and E-type specimens' exhibit similar peak loads and ductile behavior beyond the peak load except for the displacement at the peak load owing to the sliding of the displacement-measurement point. It was reported that even if the coated area represents a slight difference between the X-type and E-type specimens, the E-type coating is appropriate, as it is not sensitive to precise construction and is also suitable for the enhancement of the in-plane load-carrying capacity [24].

As indicated in Figure 7, the ductility and energy absorption capacity in the out-of-plane direction of the specimens increased in the order of +-type, X-type, and E-type reinforcements. Considering that the ductile capacity in the out-of-plane direction of the UMW is low, it was evident that the ductility and energy absorption capacity at the post-peak load were improved owing to the mechanical properties of the GFRPU. These can prevent or delay the falling off of bricks owing to the brittle characteristics of mortar during disasters.

2.5. Derivation of Formula to Describe the GFRPU Reinforcement

A bending crack is one of the fracture patterns when an out-of-plane load is applied to a masonry wall. Based on the Korean standard [25], the out-of-plane strength is calculated by dividing the cases into those in which arch action can be expected and those in which there is no arch action. When arch action can be expected:

The height-to-thickness ratio of the masonry wall is 25 or less, and arch action can be expected when it is in complete contact with the surrounding frame. The out-of-plane strength Q_{CL} is calculated as follows:

$$Q_{CL} = q_{in}A_{in} = \frac{0.7f'_m\lambda_2}{(h_m/t_m)}A_{in} \quad (1)$$

where Q_{CL} denotes the out-of-plane strength of the masonry wall (in N), q_{in} denotes the out-of-plane strength per unit area of the masonry wall (in MPa), A_{in} denotes the elevation area of the masonry wall (in mm^2), f'_m denotes the nominal compressive strength of the masonry wall, and λ_2 denotes the wall height-to-thickness ratio (Table 3).

Table 2. Correction factor for wall height-to-thickness ratio λ_2

H_m/t_m	5	10	15	25
λ_2	0.129	0.060	0.034	0.013

In this case, considering the masonry wall as a cantilever, the horizontal load is assumed to be the out-of-plane load, and the design standard tensile strength listed in Table 4 is applied. If it is confirmed through on-site investigation that there is no gap at the interface between the masonry and the frame, it is assumed that the four-sided joint is fixed.

Table 3. Height-to-thickness ratio limit value for omitting the out-of-plane examination of the masonry wall that satisfies the requirements for arch action

Performance level	S_{DS}<0.33g or S_{D1}<0.133g	0.33g≤S_{DS}<0.50g or 0.133g≤S_{D1}<0.20g	0.50g≤S_{DS} or 0.20g≤S_{D1}
Habitable	14	13	8
Life safety	15	14	9
Collapse prevention	16	15	10

* S_{DS} is 5 percent damped spectral response acceleration parameter at short period and S_{D1} 5 percent damped spectral response acceleration parameter at a period of 1second.

The out-of-plane load should be greater than the inertial force as follows:

$$F_p = 0.4\chi S_{DS}W_p \geq 0.1\chi W_p \quad (2)$$

where F_p denotes the inertial force in the out-of-plane direction, S_{DS} denotes the short-period spectral acceleration of the evaluation target earthquake considering the significance factor, W_p denotes the wall weight or unit weight, and χ denotes the coefficient according to the targeted performance level: collapse prevention: 0.3, life safety: 0.4, and habitable: 0.6 (for flexible diaphragms, values equal to three times these values is used).

If the height-to-thickness ratio of the UMW is less than the limit specified in Table 4 and satisfies the prescribed arch action, it is considered safe for in-plane overturning. In Table 4, the height-to-thickness ratio has a smaller value among the upper limits determined by S_{DS} and S_{D1}. If the height-to-thickness ratio listed in Table 4 is exceeded, the strength should be reviewed in accordance with the regulations.

The standard stipulates the design so that the masonry wall has an out-of-plane strength greater than the inertial force. The experiment indicated that the out-of-plane strength of the masonry wall was improved by the entire GFRPU reinforcement on one face. Considering the support conditions and only 80% of the peak load in the experiment, this study presented a formula to describe the out-of-plane strength of reinforced masonry walls. By including the strengthening effect owing to the support condition into Equation 1, the out-of-plane strength should be modified. It can be seen that the peak out-of-plane strength is approximately 1.5 times that used in Equation 1 specified in the standard. Thus, this work considered the GFRPU reinforcement effect, and the formula of the design criteria was modified as follows:

$$Q_{CL} = q_{in}A_{in} = \frac{1.05f_m\lambda_2}{(h_m/t_m)}A_{in} \quad (3)$$

Equation 3 represents the out-of-plane strength of the masonry wall reinforced with GFRPU. However, the formula is limited to the case where 5-mm-thick GFRPU with 5% milled glass fiber added by weight ratio is applied. Further, the effect on the spraying thickness should be considered, and its effect should be included in Equation 3. Nevertheless, the equation can be utilized based on general reinforcement by GFRPU, and it is expected that it can be applied in practice.

3. Conclusions

In this study, the strengthening effect of GFRPU reinforcement on UMWs for improving the out-of-plane strength was investigated. The effects of the coating type were compared, and a formula to express the degree of GFRPU reinforcement was proposed. Three specimens with X-type, +-type, and E-type coatings were manufactured, and a uniform static load was applied in the out-of-plane direction. Based on experiments, the following conclusions can be drawn.

- It was seen established that GFRPU could be utilized as a composite elastomer to improve the out-of-plane strength and ductility of masonry walls.
- The experiments indicated that the peak load gradually decreased in the order of X-type, E-type, and +-type specimens. Despite the prediction that the E-type specimen would demonstrate the highest loading capacity, the X-type reinforcement exhibited a higher loading capacity instead. The difference was attributed to the challenge in obtaining a uniform GFRPU dispersion and thickness on the prescribed area. Despite this difference, it was demonstrated that one-sided complete reinforcement can improve the out-of-plane strength and ductility with ease of construction and economic efficiency.
- The Korean Standard stipulates that the design of a masonry wall has an out-of-plane internal force greater than or equal to the inertial force. By modifying the expression for the out-of-plane strength specified in the Korean Standard, this study proposed an empirical formula related to the out-of-plane strength of masonry reinforced with GFRPU.
- Because the formula for estimating the out-of-plane strength is limited to the case where 5-mm-thick GFRPU with 5% added milled glass fiber by weight ratio is applied, the effect of varying the thickness should be further reviewed in future studies.

4. Declarations

4.1. Author Contributions

Conceptualization, H.C.E.; methodology, H.S.J. and S.H.S.; software, J.H.A.; validation, S.H.S., H.S.J. and Y.S.H.; formal analysis, J.H.A.; investigation, S.H.S.; resources, Y.S.H.; data curation, S.H.S.; writing—original draft preparation, H.S.J.; writing—review and editing, H.C.E.; visualization, J.H.S.; supervision, H.C.E.; project administration, H.C.E.; funding acquisition, H.C.E. All authors have read and agreed to the published version of the manuscript.

4.2. Data Availability Statement

The data used to support the findings of this study are included within the article

4.3. Funding

The authors received no financial support for the research, authorship, and/or publication of this article.

4.4. Conflicts of Interest

The authors declare no conflict of interest.

5. References

[1] Darbhanzi, A., Marefat, M. S., & Khanmohammadi, M. (2014). Investigation of in-plane seismic retrofit of unreinforced masonry walls by means of vertical steel ties. Construction and Building Materials, 52, 122–129. doi:10.1016/j.conbuildmat.2013.11.020.

[2] Lantz, L., Maynez, J., Cook, W., & Wilson, C. M. D. (2016). Blast Protection of Unreinforced Masonry Walls: A State-of-the-Art Review. Advances in Civil Engineering, 2016. doi:10.1155/2016/8958429.

[3] Myers, J. J., & Tanizawa, Y. (2010). In-plane behavior of an alternative masonry retrofitted with polyurea membranes. Structural Faults and Repair (SF&R 2010), Edinburgh, Scotland, UK.

[4] Hrynyk, T. D., & Myers, J. J. (2008). Out-of-Plane Behavior of URM Arching Walls with Modern Blast Retrofits: Experimental Results and Analytical Model. Journal of Structural Engineering, 134(10), 1589–1597. doi:10.1061/(asce)0733-9445(2008)134:10(1589).

[5] Galati, N. (2003). "Out-of-plane behavior of masonry walls strengthened with FRP materials." PhD. Dissertation. Univ. of Lecce, Lecce, Italy.

[6] Salem, S., Ezzeldin, M., El-Dakhakhni, W., & Tait, M. (2019). Out-of-Plane Behavior of Load-Bearing Reinforced Masonry Shear Walls. Journal of Structural Engineering, 145(11), 04019127. doi:10.1061/(asce)st.1943-541x.0002403.

[7] Türkmen, S., Wijte, S. N. M., De Vries, B. T., & Ingham, J. M. (2021). Out-of-plane behavior of clay brick masonry walls retrofitted with flexible deep mounted CFRP strips. Engineering Structures, 228. doi:10.1016/j.engstruct.2020.111448.

[8] Meriggi, P., de Felice, G., & De Santis, S. (2020). Design of the out-of-plane strengthening of masonry walls with fabric reinforced cementitious matrix composites. Construction and Building Materials, 240. doi:10.1016/j.conbuildmat.2019.117946.

[9] Corradi, M., Speranzini, E., & Bisciotti, G. (2020). Out-of-plane reinforcement of masonry walls using joint-embedded steel cables. Bulletin of Earthquake Engineering, 18(10), 4755–4782. doi:10.1007/s10518-020-00875-3.

[10] Guerreiro, J., Ferreira, J. G., Proença, J., & Gago, A. (2018). Strengthening of Old Masonry Walls for out-of-Plane Seismic Loading with a CFRP Reinforced Render. Experimental Techniques, 42(4), 355–369. doi:10.1007/s40799-018-0239-0.

[11] Connell, J. D. (2002). Evaluation of elastomeric polymers for retrofit of unreinforced masonry walls subjected to blast PhD. Dissertation. University of Alabama at Birmingham, United States.

[12] Broekaert, M. (2002). Polyurea spray coatings: The technology and latest developments. Paint and Coatings Industry, 18(10), 80–93.

[13] Myers, J. J. (2006). Out of Plane Behavior of Masonry Infill Walls Retrofitted With a Reinforced Polymer Grid and Polyurea ... Conference: Proceedings for the Structural Faults & Repair (2006, February 2015.

[14] Carey, N. L., & Myers, J. J. (2011). Discrete fiber reinforced polymer systems for repair of concrete structures: Polyurea-fiber characterization results. In American Concrete Institute, ACI Special Publication. Vol. 1, Issue 275 SP, 275–288.

[15] Carey, N. L., & Myers, J. J. (2010). Full scale blast testing of hybrid barrier systems. In American Concrete Institute, ACI Special Publication. Issue 281 SP, 152–170). American Concrete Institute.

[16] Greene, C. E. (2010). Compressive behavior of concrete cylinders strengthened with a discrete fiber reinforced polymer system. Doctoral dissertation, MS thesis, Missouri Univ. of Science and Technology, Rolla, MO, United States.

[17] Greene, C. E., & Myers, J. J. (2013). Flexural and Shear Behavior of Reinforced Concrete Members Strengthened with a Discrete Fiber-Reinforced Polyurea System. Journal of Composites for Construction, 17(1), 108–116. doi:10.1061/(asce)cc.1943-5614.0000308.

[18] Galati, N., Garbin, E., Tumialan, G., & Nanni, A. (2005). Design guidelines for masonry structures: Out of plane loads. American Concrete Institute, ACI Special Publication, SP-230, 269–288.

[19] Wu, G., Ji, C., Wang, X., Gao, F., Zhao, C., Liu, Y., & Yang, G. (2021). Blast response of clay brick masonry unit walls unreinforced and reinforced with polyurea elastomer. Defence Technology, 11. doi:10.1016/j.dt.2021.03.004.

[20] Song, J. H., Lee, E. T., & Eun, H. C. (2019). A Study on the Improvement of Structural Performance by Glass Fiber-Reinforced Polyurea (GFRPU) Reinforcement. Advances in Civil Engineering, 2019. doi:10.1155/2019/2818219.

[21] Song, J. H., Lee, E. T., & Eun, H. C. (2020). Shear strength of reinforced concrete columns retrofitted by glass fiber reinforced polyurea. Civil Engineering Journal (Iran), 6(10), 1852–1863. doi:10.28991/cej-2020-03091587.

[22] Song, J. H., Lee, E. T., Eun, H. C., & Apostolopoulos, C. (2020). A Study on the Strengthening Performance of Concrete Beam by Fiber-Reinforced Polyurea (FRPU) Reinforcement. Advances in Civil Engineering, 2020. doi:10.1155/2020/6967845.

[23] Song, J. H., & Eun, H. C. (2021). Improvement of flexural and shear strength of RC beam reinforced by glass fiber-reinforced polyurea (GFRPU). Civil Engineering Journal (Iran), 7(3), 407–418. doi:10.28991/cej-2021-03091662.

[24] Son, S. H. (2021). A study on in-plane strengthening effect of masonry wall by composite material of milled glass fiber and polyurea. PhD Thesis, Kangwon National University, Korea.

[25] Korea Facilities Safety Corporation. (2019). Seismic performance evaluation guidelines for existing facilities. Buildings, Korea.